

Hierarchy Crystallization Structure of a Polypropylene Random Copolymer Injection-Molded Bar Induced by a Nucleating Agent

Yong Wang, Yao Gao, Jing Shi

Key Laboratory of Advanced Technologies of Materials (Ministry of Education), School of Materials Science and Engineering, Southwest Jiaotong University, Chengdu 610031, China

Received 12 March 2007; accepted 11 July 2007

DOI 10.1002/app.27121

Published online 13 September 2007 in Wiley InterScience (www.interscience.wiley.com).

ABSTRACT: In this work, the effect of a nucleating agent on the crystallization structure of an injection-molded bar of a polypropylene random copolymer (PPR) with sorbitol derivatives [1,2,3,4-dibenzylidene sorbitol (DBS)] has been studied. The results show that pure PPR forms a simple skin-core crystallization structure. However, PPR/DBS forms an interesting and complicated hierarchy crystallization structure: there is a transition layer between the skin layer and the core zone. In this transition layer, the crystallization structure consists of some perfect spherulites and many tiny crystallites. Further research suggests that the formation of the hierarchy crystallization structure depends on not only the content of the nucleating agent in the PPR

matrix but also the mold temperature during the injection-molding processing. The crystallization behavior of PPR/DBS during the cooling process has been characterized with polarization optical microscopy and differential scanning calorimetry. The results suggest that there are different mechanisms in the crystallization process of PPR/DBS. The formation of a three-dimensional DBS network under a certain condition might be the main reason for the complicated hierarchy crystallization structure. © 2007 Wiley Periodicals, Inc. *J Appl Polym Sci* 107: 309–318, 2008

Key words: crystal structures; nucleation; poly(propylene) (PP)

INTRODUCTION

The hierarchy structure of injection-molded bars has been intensively researched in the last 10 years because the multiple layers are very important for the end-use properties of the molded articles. During injection-molding processing, the wall temperature of the mold is much lower than that of the polymer melt. The solidifying rate of the melt that is in contact with the mold wall is higher than that of the melt that is far away from the mold wall. Macroscopically, the injection-molded bar has an apparent hierarchy structure, that is, a skin-core structure. In the different layers of an injection-molded bar, the bar shows different morphologies. For example, in the skin layer of a polypropylene (PP)/linear low-density polyethylene (50/50) injection-molded bar obtained with a high injection speed and high pressure, a homogeneous phase morphology is observed because the

homogeneous melt is frozen by the fast solidifying process. However, in the core zone, a cocontinuous two-phase structure is observed because of the phase dissolution at a lower solidifying rate.¹

So far, research on the hierarchy or anisotropic structure of polymer injection-molded bars has been mainly focused on semicrystalline polymers and their blends, such as PP. The hierarchy structure of PP injection-molded bars has been characterized with different methods: light microscopy,^{2–5} small-angle X-ray scattering,^{6–9} and wide-angle X-ray scattering.^{2–3,8–10} Much work has been done to research the effects of shear stress on the crystallization structure and orientation texture of PP obtained during injection-molding processing.^{2–10} For example, in the skin layer of an injection-molded PP bar, the orientation of PP is quite apparent, and some shish or shish-kebab structure is observed. However, in the core zone, the oriented PP macromolecules will be relaxed, and the shish-kebab structure can be changed into a kebab structure or random crystalline lamellae.⁶

Nucleating agents are widely used in thermoplastic polymer processing because they have the abilities to increase the crystallization speed of these semicrystalline polymers, reduce the cycle time, and improve the optical properties apparently. Among all nucleating agents, sorbitol derivatives are thought

Correspondence to: Y. Wang (yongwang1976@163.com).

Contract grant sponsor: Alexander von Humboldt Foundation (Germany).

Contract grant sponsor: Sichuan Youthful Science and Technology Foundation (China); contract grant number: 07ZQ026-003.

Journal of Applied Polymer Science, Vol. 107, 309–318 (2008)
© 2007 Wiley Periodicals, Inc.

to be some of the most efficient nucleating agents for PP crystallization because they crystallize into nanofibrillar structures in the polymer melt through self-organization.^{11–15} Previous research results have shown that the formation of sorbitol fibrils depends on both the concentration of sorbitol in the matrix and the temperature of the melt. A high content of sorbitol and a low melt temperature are in favor of the formation of a three-dimensional (3D) sorbitol network.¹⁵ Some work has been done to research the formation mechanism of sorbitol networks and its effects on PP crystallization behaviors, especially on the formation of the anisotropic structure.^{16–18}

As a part of serial work on the crystallization behavior of semicrystalline polymers induced by a nucleating agent, in this study, we researched the crystallization structure of a polypropylene random copolymer (PPR) with a nucleating agent directly. Because the crystallization structure is related to the transparency or clarity of the sample, our attention was focused on the study of the crystallization structure that is formed during the injection processing. Only 0.10 or 0.20 wt % 1,2,3,4-dibenzylidene sorbitol (DBS) was added to PPR, and different mold temperatures were set for PPR injection-molding processing to research the effects of the nucleating agent content and mold temperature on the crystallization structure of injection-molded bars. It was also expected that the results would be in favor of understanding the formation mechanism of the 3D sorbitol network and its effect on the crystallization structure of PPR injection-molded bars. The crystallization structure in different zones of injection-molded bars was characterized with a light microscope. A complicated hierarchy crystallization structure, in which there was a transition layer with some perfect spherulites and many tiny crystallites between the skin layer and core zone, was observed for a PPR injection-molded bar with 0.10 wt % DBS. However, only a simple skin–core crystallization structure was observed in a pure PPR injection-molded bar, and a homogeneous crystallization structure was observed in a PPR injection-molded bar with 0.20 wt % DBS.

EXPERIMENTAL

Materials

Both the PPR and nucleating agent were commercially available. PPR 3260, obtained from Total Petrochemical Co. (Carling-Saint-Avold, France), was a random copolymer of PP with 3 mol % polyethylene. The melt flow rate of PPR was 1.8 g/10 min (230°C/2.16 kg), and the density was 0.902 g/cm³. A master batch of 10 wt % DBS (Igraclear D) in Moplen HP500N was obtained from Ciba (Basel, Switzerland). Although a master batch of Moplen HP500N

(another grade of PP) was used in this work, it might have affected the crystallization behavior of PPR (e.g., Moplen HP500N as a heterogeneous nucleus of PPR). However, the heterogeneous nucleation role of DBS was more efficient than the nucleation role of PP, and in this condition, the crystallization structure of PPR was mainly affected by DBS rather than PP.

Sample preparation

PPR with different contents of DBS (PPR010 and PPR020 with weight fractions of 0.10 and 0.20 wt %, respectively) was blended with a twin-screw extruder (ZSK30, Werner & Pfleiderer, Dinkelsbuehl, Germany). During the extrusion processing, the melt temperature was 200°C, and the temperature of the die was 215°C. The rotation speed of the extruder screw was 300 rpm, and the throughput was 7 kg/h. After pellets were made, the material was dried for 4 h at the temperature of 60°C. Then, the pellets were injection-molded with an injection machine (FX75-2F, Klöckner Ferromatik Desma, Malterdingen, Germany). During the injection processing, the melt temperature of PPR was 225°C, and the mold temperature was set as follows: 60, 80, and 110°C.

Polarization optical microscopy (POM) measurements

To research the crystallization structure that formed during the injection-molding processing, a Leitz (Oberkochen, Germany) microtome was used to cut a slice from the injection-molded bar perpendicularly to the flow direction. During the cutting process, the sample and the knife were cooled with liquid nitrogen. The thickness of the sample slice was 8 μm. The sample slice was placed between two glass slices, and the crystallization structure was characterized with an Orthoplan polarization optical microscope (Leitz). In this work, two different zones of the sample were researched: the edge of the sample slice and the core zone of the sample slice. A schematic of the sample slice is shown in Figure 1.

The formation of nuclei and the growth of spherulites of PPR010 were also characterized via POM with a Mettler (Greifensee, Switzerland) FP82 hot stage (with a Mettler FP80 central processor). At first, a sample was placed between two glass slices and was heated to complete melting; then, the sample was transferred into the hot stage with the setting temperature of 140°C and kept at that temperature for 2 min. Then, the temperature of the hot stage was decreased to 80°C at the cooling rate of –2°C/min. A Leica (Wetzlar, Germany) DC 200 was used to record the nucleation and growth of the crystallization structure. To eliminate the effect of

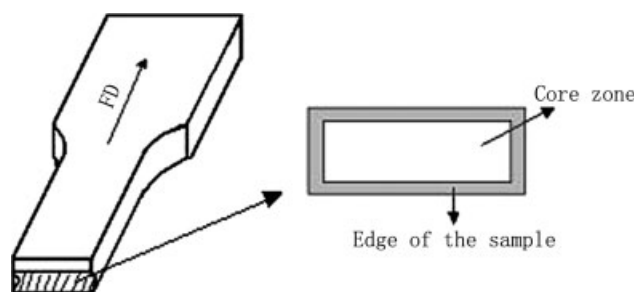


Figure 1 Schematic of a sample slice cut from an injection-molded bar for POM research. The arrow represents the flow direction (FD).

the sample thickness on the size of the spherulites, a piece of polyimide film (with a thickness of 50 μm) with a circle hole was placed between two glass slices, and the sample was placed at the center of the hole, which could guarantee that the thickness of the sample was always 50 μm .

Differential scanning calorimetry (DSC) measurement

A PerkinElmer (Waltham, MA) DSC-7 was used to research the nonisothermal crystallization behavior of PPR010. The weight of the sample was about 5 mg. The DSC scanning program was set as follows: first, the sample was heated from 50 up to 200°C at the heating rate of 20°C/min and was maintained at 200°C for 5 min to erase the thermal history; second, the sample was quenched to 140°C quickly and maintained at this temperature for 2 min; and third, the sample was cooled to 80°C at the cooling rate of $-2^\circ\text{C}/\text{min}$. During the scanning procedure, the experiment was carried out in a nitrogen atmosphere.

RESULTS

Effect of the nucleating agent content

The crystallization structure of pure PPR that formed during the injection-molding processing is shown in Figure 2. Figure 2(a,b) shows the typical crystallization structure in the skin layer and the core zone of the bar obtained at the mold temperature of 110°C, respectively. Figure 2(c) shows the crystallization structure in the core zone with a higher magnification. Apparently, for pure PPR, big spherulites can be observed in the core zone of the injection-molded bar. With the higher magnification, very perfect spherulites can be observed, and the diameters of the spherulites are about 10–30 μm . However, in the skin layer, very small spherulites can be observed. It is very difficult to calculate the diameter of the spherulites. The injection-molded bar apparently has a skin–core crystallization structure, and the thickness of the skin layer is about 200 μm . It is easy to understand. During the injection processing, the wall

temperature is much lower than that of the polymer melt. The melt that is in contact with the mold wall has a higher cooling rate, which induces a higher nucleation density in this zone. However, in the melt that is far away from the mold wall, for example, in the core zone of the bar, the melt has a much lower

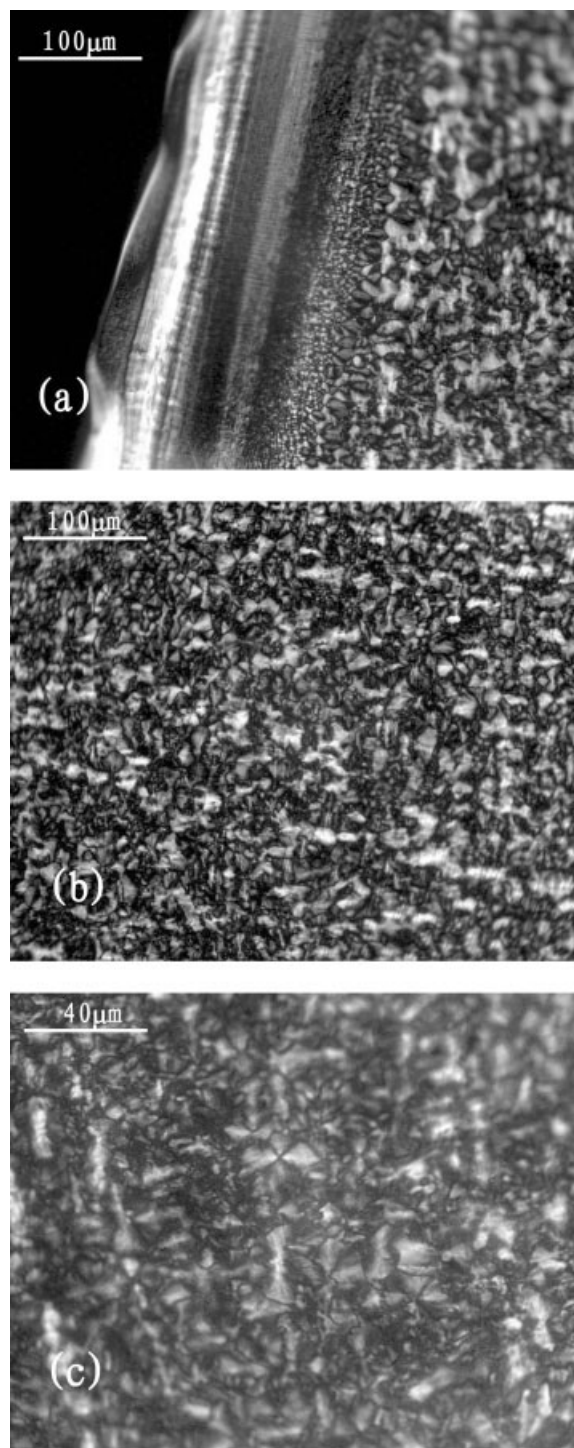


Figure 2 POM photographs of crystallization structures of a pure PPR injection-molded bar: (a) skin layer, (b) core zone, and (c) core zone with higher magnification.

cooling rate, which induces a lower nucleation density. The different nucleation densities result in different crystallization structures in the whole bar: a large number of very small spherulites (or tiny crystallites) form in the skin layer, and fewer but more perfect spherulites form in the core zone. The same results can be seen in other researchers' work.²

However, for PPR010, a more interesting crystallization structure can be observed (see Fig. 3). In the part of the bar that is in contact with the mold wall, very small spherulites can be observed. The same crystallization structure can also be observed in a pure PPR bar. The thickness of this part is about 100 μm , and it is the skin layer of the injection-molded bar. From 100 to 300 μm (calculated from the skin layer to the core zone), much bigger spherulites can be observed, and the spherulites size is up to 25 μm . Furthermore, along the arrow direction, the number of these perfect spherulites decreases gradually. Meanwhile, in this part, besides the isolated and perfect spherulites, many tiny crystallites can also be observed. The whole crystallization structure includes some perfect spherulites and many tiny crystallites. In the core zone, the spherulites are very small, and the size dispersion is very uniform; it is difficult to differentiate the spherulites one by one. Apparently, in this bar, between the skin layer and the core zone, there is a transition layer, in which the crystallization structure is different from the one in the skin layer or in the core zone.

It is interesting to make a comparison between PPR injection-molded bars and PPR010 injection-molded bars. In the skin layers, the same crystallization structures can be observed in both bars. In the core zones, the average diameters of PPR010 spherulites are much smaller than those of pure PPR spherulites. It is known to all that sorbitol derivatives are thought to be one group of remarkably efficient nucleating agents for PP crystallization; the addition of only small amounts (~ 0.20 wt %) to the polymer induces a great increase in the nucleation density and an enhancement of the crystallization temperature.¹¹⁻¹⁴ During the injection-molding processing, in the core zone of a pure PPR bar, the crystallization of PPR is a homogeneous nucleation process that results in a smaller nucleation density and finally results in the formation of perfect spherulites. Once DBS is in the melt, the crystallization of PPR is a heterogeneous nucleation process. The much higher nucleation density results in the formation of a large number of tiny crystallites. The most interesting phenomenon is that, for pure PPR, the injection-molded bar shows the simple skin-core structure. Very small spherulites and much bigger spherulites can be observed in the skin layer and in the core zone, respectively. However, for PPR010, the injection-molded bar shows a complicated crystallization

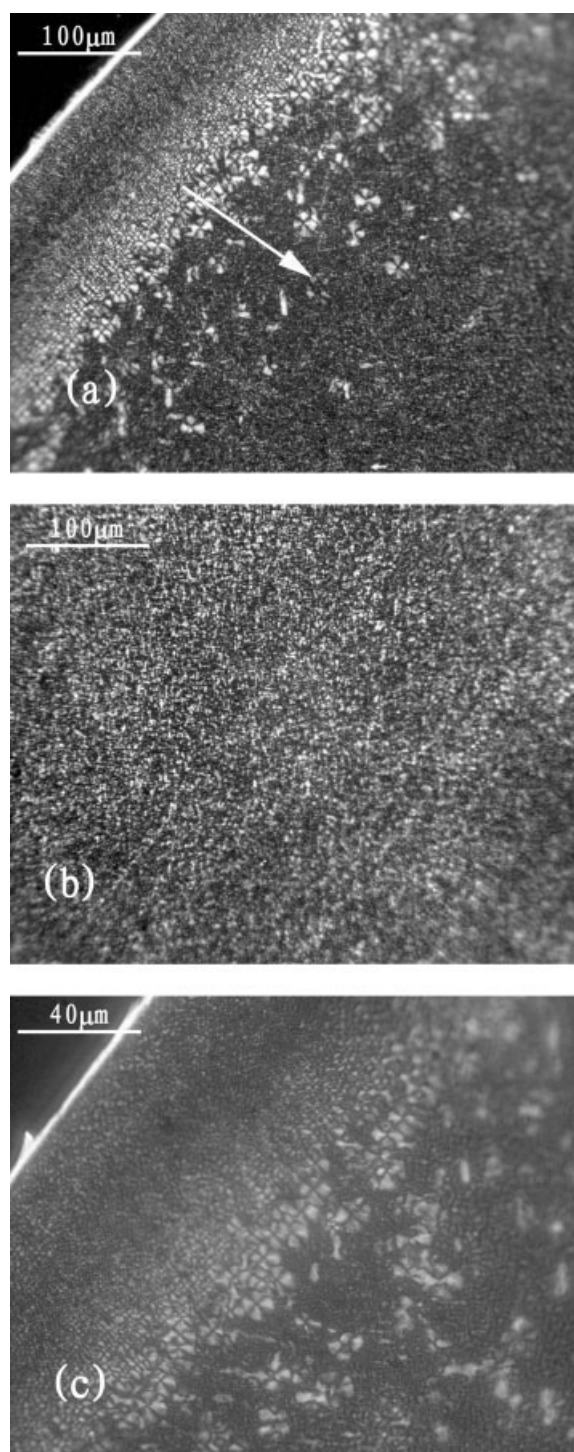


Figure 3 POM photographs of crystallization structures of PPR010: (a) skin layer, (b) core zone, and (c) skin layer under higher magnification.

structure, and the whole bar has at least three different sections: the skin layer, the transition layer, and the core zone.

To further understand the formation mechanism of this complicated crystallization structure, more DBS was added to the PPR matrix. The crystallization

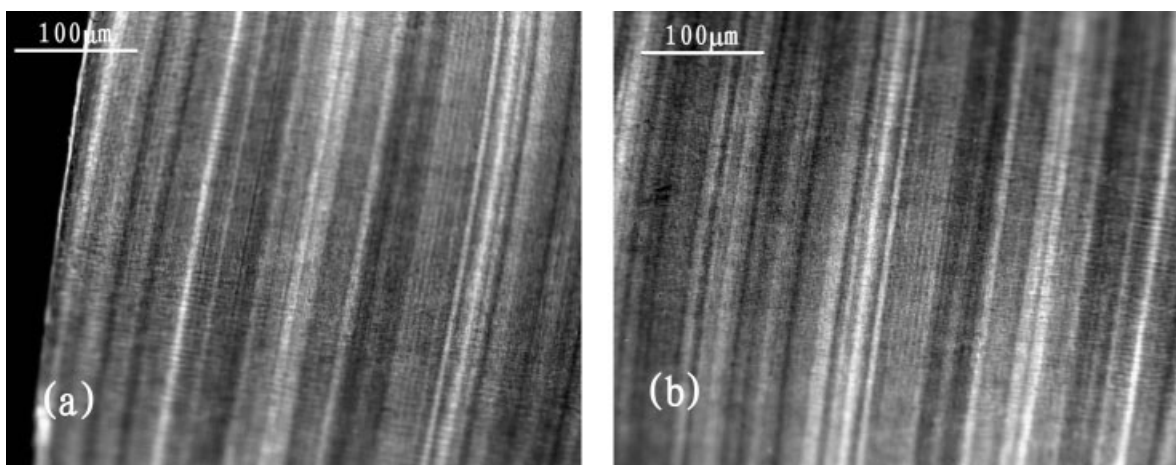


Figure 4 POM photographs of crystallization structures of PPR020: (a) skin layer and (b) core zone.

structure of a PPR injection-molded bar with a higher content of DBS (0.20 wt %) is shown in Figure 4. The whole bar shows a uniform crystallization structure whether in the skin layer or in the core zone. Figure 4 suggests that the nucleation role of DBS (0.20 wt %) is very apparent and that the nucleation density is much higher than that of pure PPR during the crystallization. The DSC results prove that the crystallization temperature of PPR is enhanced from 105.2°C for pure PPR to 115.9°C for PPR020 at the cooling rate of $-10^{\circ}\text{C}/\text{min}$ (not shown here). The crystallization rate is very high, and the whole sample forms a uniform crystallization structure in a very short time.

On the other hand, the thickness of the skin layer is reduced from 200 μm for PPR to 100 μm for PPR010 and 0 μm for PPR020. In PPR020, it is difficult to differentiate the skin layer and the core zone from the injection-molded bar, and the bar has a uniform crystallization structure instead of a hierarchy crystallization structure. The reduction of the skin-layer thickness suggests that the addition of DBS redounds to the formation of a macroscopically uniform injection-molded bar.

Effect of the mold temperature

Apparently, a hierarchy crystallization structure forms in pure PPR and PPR010 bars, especially for PPR010; that injection-molded bar has a complicated hierarchy crystallization structure. To further understand the formation of the hierarchy crystallization structure of PPR010, different mold temperatures were set for PPR010 injection-molding processing to provide different crystallization conditions. The variation of the mold temperature means a change in the cooling rate of the melt. Figures 5 and 6 show the crystallization structures in the skin layer and in the core zone of PPR010 injection-molded bars obtained

at different mold temperatures, respectively. For a clear comparison of the crystallization structures, the crystallization structures of PPR010 obtained at the mold temperature of 110°C are also shown in Figures 5 and 6. For the section near the edge of the bars, the crystallization structures obtained at mold temperatures of 60 and 80°C are apparently different from the crystallization structure of PPR010 obtained at 110°C. The skin layers are more apparent at lower mold temperatures, and their thickness is about 200 μm . On the other hand, we can still observe a very thin section (with a thickness of 50 μm) between the skin layer and the core zone of the injection-molded bar that was molded at 80°C, in which some perfect but small spherulites can be observed, and the bar still has the hierarchy crystallization structure: skin layer, transition layer, and core zone. However, a simple skin-core structure can be observed for the PPR010 bar molded at 60°C.

In the core zone, the crystallization structure of PPR010 obtained at 80°C is nearly the same as the one obtained at 110°C, and this means that there is the same crystallization mechanism. Furthermore, some white dots can be observed in the POM images, and these white dots represent some bigger spherulites. Although these spherulites are still very small, it can be deduced that there are different crystallization mechanisms for the different crystallization structures of PPR010 at the mold temperature of 80°C. It is interesting to observe that these isolated spherulites become greater with a decrease in the mold temperature. At 60°C, more white dots can be observed in the POM image, and this means that more big spherulites form during the solidifying process. Generally, at a lower temperature, the nucleation density is higher than that at a higher temperature. The decrease in the mold temperature represents an increase in the cooling rate during the injection processing, and this induces the increase in

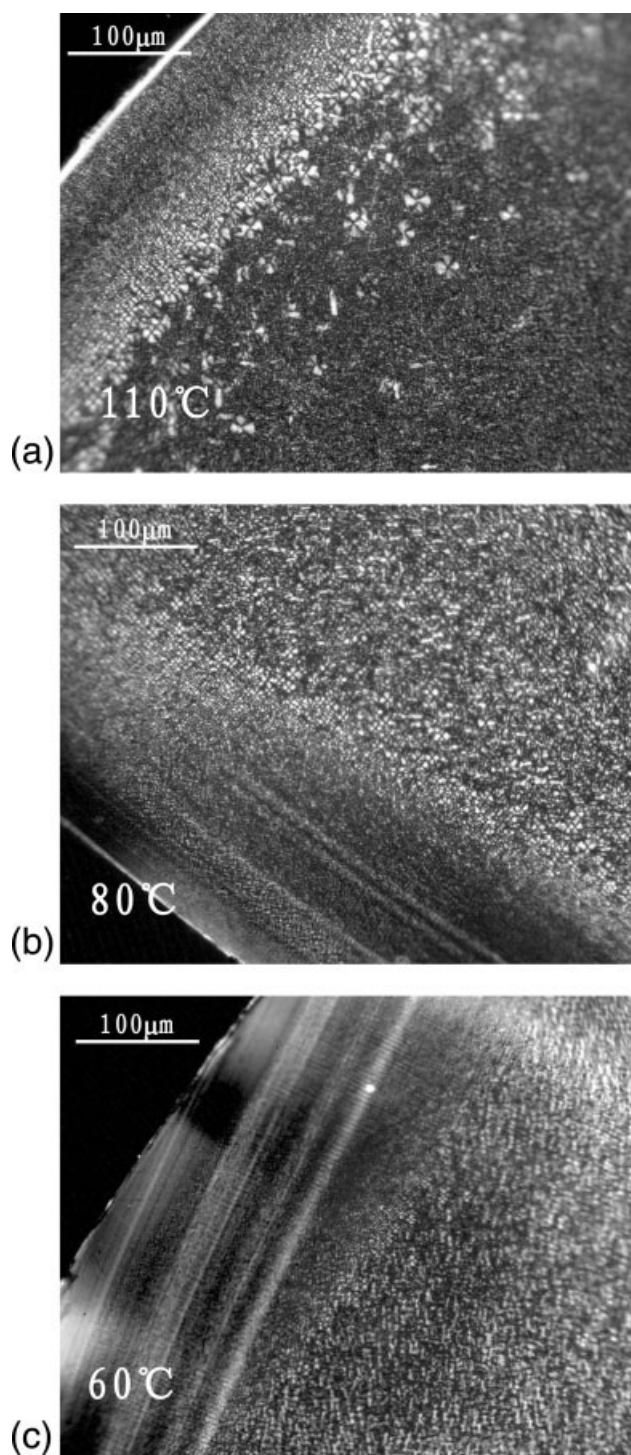


Figure 5 POM photographs of the crystallization structures in the skin layer of PPR010 obtained at different mold temperatures.

the nucleation density and finally results in the decrease in the spherulite size. However, in this work, contrary results were obtained when DBS was added to PPR. More and bigger spherulites were obtained in the core zone of the injection-molded bar at a lower mold temperature. Apparently, these

special crystallization structures are induced by a special crystallization mechanism. This is discussed in detail in the next part.

The schematics of the hierarchy crystallization structures of the injection-molded bars of PPR and

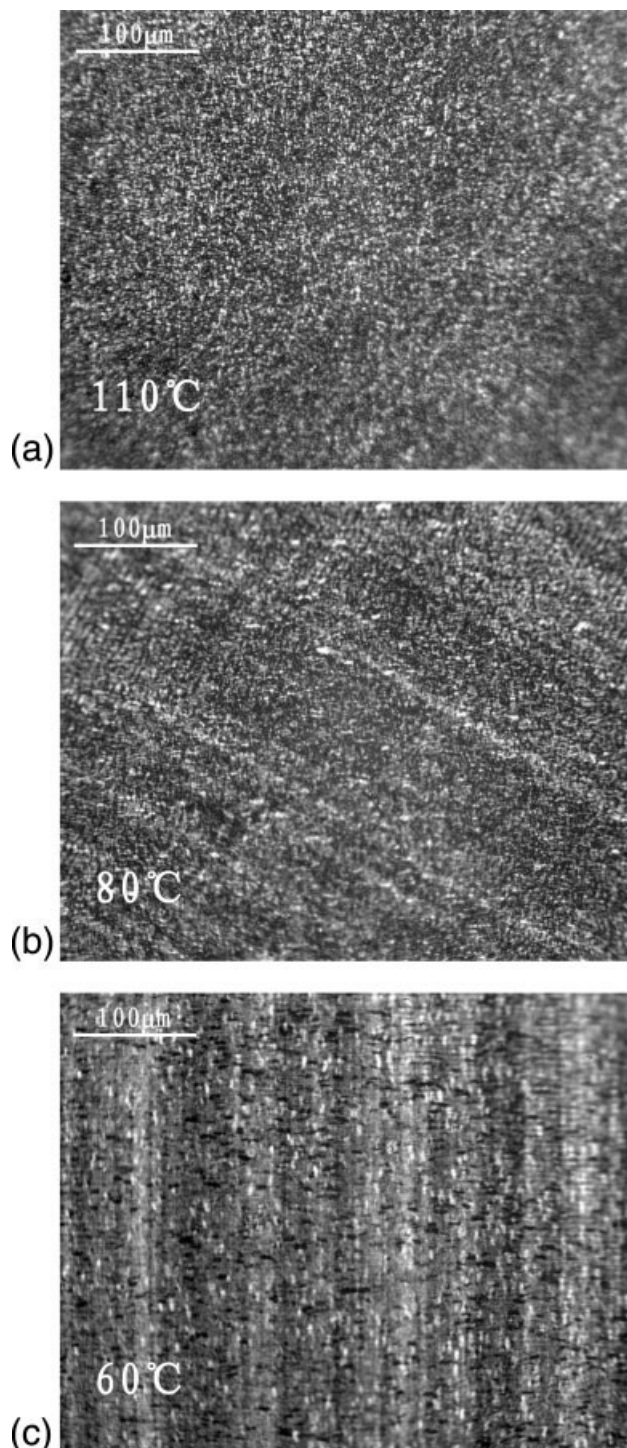


Figure 6 POM photographs of the crystallization structures in the core zone of PPR010 obtained at different mold temperatures.

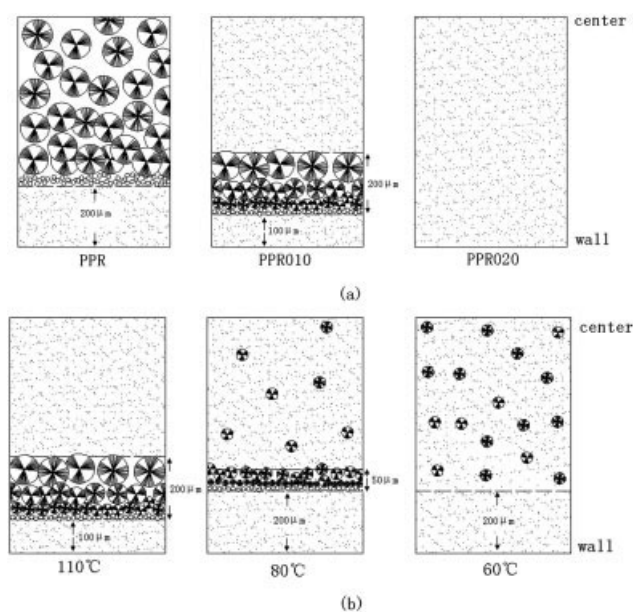


Figure 7 Schematic of the hierarchy crystallization structures of a PPR injection-molded bar: (a) the effect of the DBS content on the hierarchy crystallization structure and (b) the effect of the mold temperature on the PPR010 hierarchy crystallization structure.

PPR with DBS are shown in Figure 7, and these schematics help us to understand the formation of the hierarchy crystallization structure of PPR in this work.

DISCUSSION

The aforementioned results show that the addition of 0.10 wt % DBS leads to the formation of a complicated hierarchy structure in the injection-molded bar during injection-molding processing. Besides the skin layer and the core zone, there is a transition layer in which PPR forms more perfect and bigger spherulites. The formation of this hierarchy crystallization structure is affected by the content of DBS in PPR and the mold temperature during the injection processing. The aforementioned results also suggest that there are different mechanisms for the crystallization of PPR010. To understand the formation mechanism of the hierarchy crystallization structure, the evolution of the crystallization structure during the cooling process was recorded with POM, and the nonisothermal crystallization behavior was analyzed with DSC.

Figure 8 shows the POM photographs of PPR010 crystallization structures obtained at the cooling rate of $-2^{\circ}\text{C}/\text{min}$, and these photographs were taken at different temperatures. At 122.8°C , very small isolated spherulites could be seen. This is the initial stage of the crystallization, and the whole crystalliza-

tion rate depends on the nucleation rate. With decreasing temperature, these isolated spherulites grow further, and the number of these spherulites also increases. On the other hand, a new crystallization phenomenon can be seen in the POM images. A cluster of tiny crystallites appears at a lower temperature (as shown by an arrow). The number of the cluster becomes greater, and the size of the cluster increases greatly at 119.0°C ; this means that the crystallization rate increases greatly. At 116.9°C , the crystallization of PPR010 is nearly finished. Two different crystallization structures coexist in the system: one consists of isolated spherulites with bigger diameters, and the other is a cluster of tiny crystallites. Obviously, the latter dominates the final crystallization structure. From the evolution of the PPR010 crystallization structure, it can be seen that the formation of the cluster is later than that of the isolated spherulites. In other words, the formation of the cluster needs a longer induction time than the isolated spherulites. Once the cluster appears, it grows very fast and dominates the final crystallization structure.

The DSC cooling curve of PPR010 is shown in Figure 9(a). From the shape of the crystallization peak, it also can be seen that in the initial stage, the crystallization is very slow. When the temperature decreases down to 112.3°C , the crystallization rate increases greatly. In a very short time, the crystallization of PPR010 is finished.

Normally, the isothermal crystallization of a polymer can be described by the Avrami equation,^{19,20} and this method is not precise for describing nonisothermal crystallization. Some other new methods have been developed, such as Ozawa's theory²¹ and Mo's theory.²² However, in this work, we still use the Avrami method to show the crystallization mechanism during the cooling process:

$$1 - X_t = \exp(-Kt^n) \quad (1)$$

where X_t is the relative degree of crystallinity at time t ; n is the Avrami exponent, which depends on the type of nucleation and growth mechanism during the crystallization; and K is the rate constant, which also depends on the nucleation and growth mechanism in actual circumstances. According to the Avrami equation, the formula can be written as follows:

$$\lg[-\ln(1 - X_t)] = n \lg t + \lg K \quad (2)$$

Generally, a plot of $\lg[-\ln(1 - X_t)]$ versus $\lg t$ is a straight line. The slope of the line is n , and the intercept is $\lg K$.

Figure 9(b) shows a plot of $\lg[-\ln(1 - X_t)]$ versus $\lg t$ of PPR010 at the cooling rate of $-2^{\circ}\text{C}/\text{min}$. The plot is not a simple straight line but is a curve with

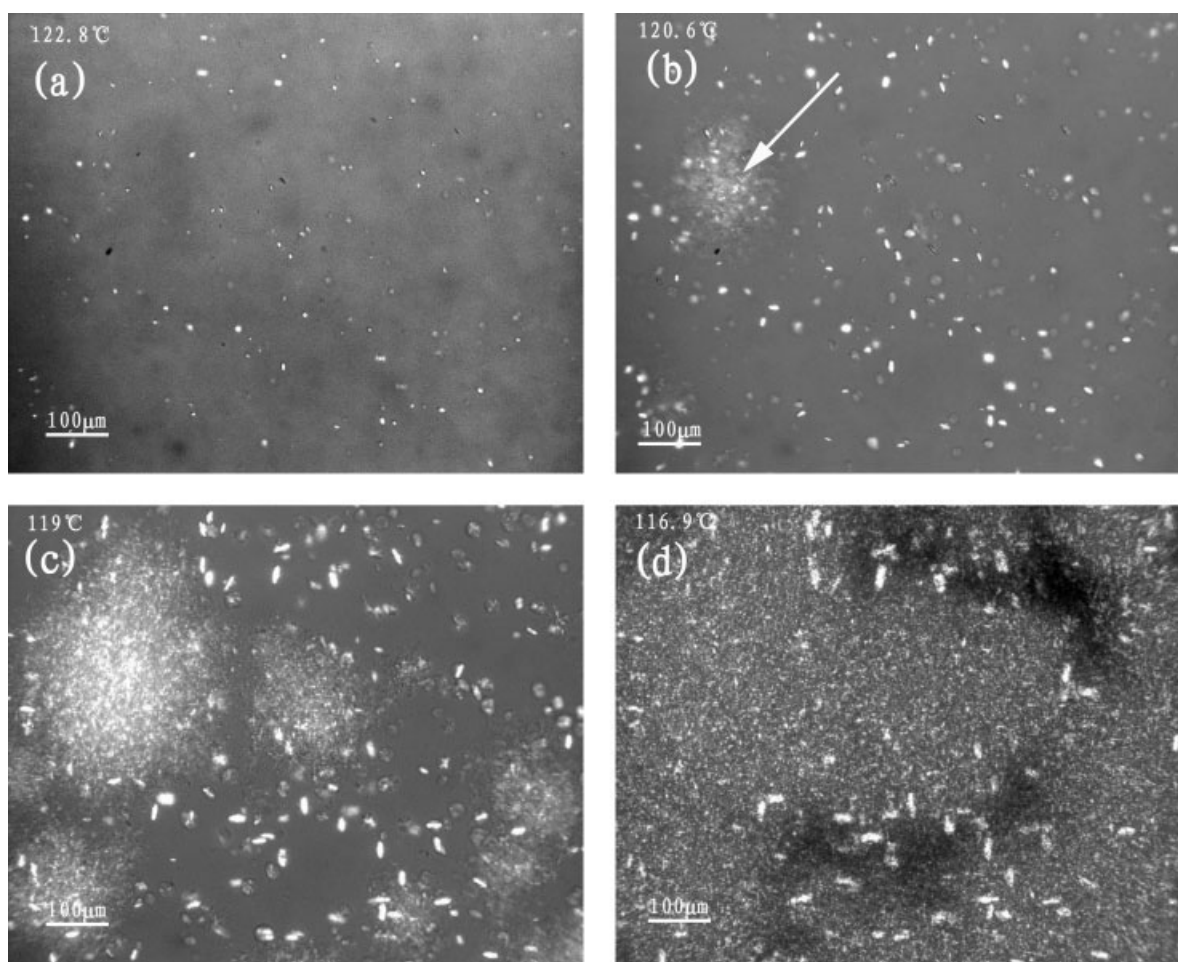


Figure 8 Growth of the crystallization structure of PPR010 at a cooling rate of $-2^{\circ}\text{C}/\text{min}$. The POM photographs were taken at different temperatures: (a) 122.8, (b) 120.6, (c) 119.0, and (d) 116.9 $^{\circ}\text{C}$.

two steps. The curve shows an initial linear portion and subsequently tends to level up to another linear portion. The result is totally different from the previous results in the literature.²³ The first linear portion of the plot is thought to be the result of the primary crystallization, but the deviation of the plots suggests that some new nucleation behavior takes place during the crystallization. If we suppose that the two steps of crystallization can be analyzed by the Avrami equation, the values of $\lg K$ and n can be calculated as follows: in the earlier stage, $\lg K_1$ and n_1 are -6.41 and 2.79 , respectively. This means that the growth of crystallization is a 3D growth mechanism. However, in the later stage, $\lg K_2$ and n_2 are -11.31 and 5.10 , respectively. The variation of $\lg K$ and n proves the great increase in the crystallization rate of PPR010 in the later stage. In the earlier stage, the nucleation is heterogeneous, and n is independent of the crystallization time. The whole crystallization rate of PPR depends on not only the nucleation of PPR induced by DBS but also the growth of existing spherulites. However, in the later stage of the

PPR010 crystallization process, besides the further growth of existing spherulites, a new cluster of crystallites appears and grows greatly. Therefore, $\lg K_2$ and n_2 show not only the nucleation and growth of those bigger spherulites but also the formation and growth of the new clusters of those tiny crystallites. It is well known that sorbitol derivatives can form a so-called 3D network in the polymer melt when the content of sorbitol derivatives reaches a critical value.^{15–18} According to our results, we believe that there might be some 3D networks of DBS in the melt and that they induce PPR crystallization in a very short time in the later stage of the PPR010 crystallization process. The effect of this 3D network of sorbitol derivatives on PPR crystallization behavior and its formation mechanism will be discussed in our further work.

The study of the crystallization evolution and non-isothermal crystallization kinetics shows that, during the cooling process, the crystallization rate is increased greatly in the later stage of PPR010 crystallization, and this could be attributed to the forma-

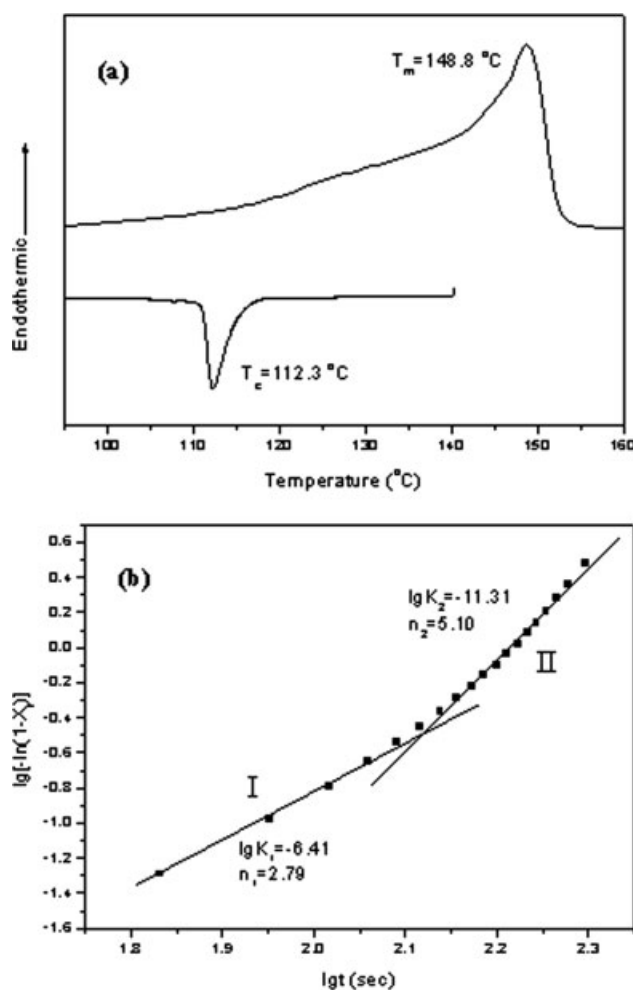


Figure 9 DSC measurements of PPR010: (a) heating and cooling curves of PPR010 during the DSC measurements and (b) an Avrami plot of PPR010 obtained at the cooling rate of $-2^\circ\text{C}/\text{min}$ (T_m = melting temperature; T_c = crystallization temperature).

tion of a 3D sorbitol network. Now it is easy to understand why a more complicated hierarchy crystallization structure forms in the injection-molded bar. During the injection processing, once the PPR010 melt contacts the mold wall, the temperature of the melt decreases quickly, and this induces the formation of many tiny crystallites in the skin layer. Under this condition, the time is too short for DBS to form the 3D network; the crystallization of PPR is mainly induced by dispersed DBS fibrils. However, from the skin layer to the core zone, the cooling rate decreases gradually. Near the skin layer, some isolated spherulites, which are induced by dispersed DBS fibrils, grow at a lower supercooling degree (higher temperature), and these spherulites grow very fast with the decrease in the temperature. In the core zone, the temperature decreases very slowly, and the lower supercooling degree (higher temperature) does not favor the nucleation of PPR.

However, the lower supercooling degree allows enough induction time for the formation of a 3D sorbitol network. Once DBS forms the network structure, it increases the nucleation density greatly, induces PPR crystallization in a very short time, and finally results in the formation of a crystallization structure with tiny crystallites.

At a lower mold temperature, in the core zone of the injection-molded bar, the crystallization is induced by dispersed DBS fibrils before the formation of a 3D DBS network, and this results in the formation of isolated spherulites; the number of these isolated spherulites increases with a decrease in the mold temperature. Once DBS forms the 3D network in the PPR melt, it induces PPR crystallization in a very short time. That is why at a lower mold temperature (80 or 60°C), the crystallization structure includes some isolated bigger spherulites and many tiny crystallites in the core zone of the injection-molded bar.

For PPR020, because of the relatively high content of DBS, it is easy for DBS to form the 3D network in the bar whether near the mold wall or far away from the mold wall, and the crystallization of PPR is dominated by the 3D DBS network. The higher concentration of the 3D network results in the formation of the uniform crystallization structure with tiny crystallites in the whole injection-molded bar.

CONCLUSIONS

In summary, the hierarchy crystallization structures of PPR/DBS injection-molded bars have been researched with POM and DSC methods. The results show that the addition of a little DBS (0.10 wt %) induces PPR to form a complicated hierarchy crystallization structure: there is a transition layer that includes some perfect spherulites and many tiny crystallites between the skin layer and the core zone. The formation of the transition layer depends on not only the content of DBS in the PPR matrix but also the mold temperature (supercooling degree). Further research suggests that the formation of the hierarchy crystallization structure in this work is the result of different crystallization mechanisms. For PPR010, because of the higher cooling rate (higher supercooling degree) and shorter induction time, PPR crystallization is mostly induced by dispersed DBS fibrils in the skin layer; in the transition layer, two different crystallization mechanisms coexist: one is the crystallization induced by DBS fibrils, and the other one is the crystallization induced by a 3D DBS network. In the core zone, the crystallization of PPR is mainly induced by the 3D network of DBS.

Bernd-J. Jungnickel and Hans Kothe (Deutsches Kunststoff-Institut) are greatly appreciated for useful discussion.

References

1. Wang, Y.; Zou, H.; Fu, Q.; Zhang, G.; Shen, K. Z.; Thomann, R. *Macromol Rapid Commun* 2002, 23, 749.
2. Kantz, M. R.; Newman, H. D.; Stigale, F. H. *J Appl Polym Sci* 1972, 16, 1249.
3. Kalay, G.; Bevis, M. J. *J Polym Sci Part B: Polym Phys* 1997, 35, 265.
4. Kumaraswamy, G.; Kornfield, J. A.; Yeh, F.; Hsiao, B. S. *Macromolecules* 2002, 35, 1762.
5. Fitchmun, D. R.; Mencik, Z. *J Polym Sci Polym Phys Ed* 1973, 11, 951.
6. Zhu, P. W.; Edward, G. *Polymer* 2004, 45, 2603.
7. Zhu, P. W.; Edward, G. *Macromolecules* 2004, 37, 2658.
8. Kumaraswamy, G.; Verma, R. K.; Kornfield, J. A.; Yeh, F.; Hsiao, B. S. *Macromolecules* 2004, 37, 9005.
9. Wang, Y.; Na, B.; Fu, Q.; Men, Y. F. *Polymer* 2004, 45, 207.
10. Zipper, P.; Janosi, A.; Geymayer, W.; Ingolic, E.; Fleischmann, E. *Polym Eng Sci* 1996, 36, 467.
11. Thierry, A.; Straupe, C.; Lotz, B.; Wittmann, J. C. *Polym Commun* 1990, 31, 299.
12. Fillon, B.; Lotz, B.; Thierry, A.; Wittmann, J. C. *J Polym Sci Part B: Polym Phys* 1993, 31, 1395.
13. Marco, C.; Ellis, G.; Gomez, M. A.; Arribas, J. M. *J Appl Polym Sci* 2003, 88, 2261.
14. Kristiansen, M.; Werner, M.; Tervoort, T.; Smith, P. *Macromolecules* 2003, 36, 5150.
15. Shepard, T. A.; Delsorbo, C. A.; Louth, R. M.; Walborn, J. L.; Norman, D. A.; Harvey, N. G.; Spontak, R. A. *J Polym Sci Part B: Polym Phys* 1997, 35, 2617.
16. Nogales, A.; Mitchell, G. R. *Macromolecules* 2003, 36, 4898.
17. Nogales, A.; Mitchell, G. R. *Polymer* 2005, 46, 5615.
18. Nogales, A.; Olley, R. H.; Mitchell, G. R. *Macromol Rapid Commun* 2003, 24, 496.
19. Avrami, M. *J Chem Phys* 1940, 8, 212.
20. Jeziorny, A. *Polymer* 1978, 19, 1142.
21. Ozawa, T. *Polymer* 1971, 12, 150.
22. Liu, T. X.; Mo, Z. S.; Wang, S. E. *Polym Eng Sci* 1997, 37, 568.
23. Huang, Y. P.; Chen, G. M.; Yao, Z.; Li, H. W.; Wu, Y. *Eur Polym J* 2005, 41, 2753–2760.